Lattice location of I implanted into Fe single crystals*

P. T. Callaghan,[†] P. K. James, and N. J. Stone

Clarendon Laboratory, University of Oxford, England

(Received 4 February 1975)

The channeling technique has been used to locate I atoms implanted at 140 keV into Fe single crystals with a dose of 5×10^{14} atoms cm^{-2}. Observations were made of the backscattering yield for 3.5-MeV ^{14}N ions in angular scans across the $\langle 111 \rangle$, $\langle 110 \rangle$ axial, and $\{110\}, \{100\}$, and $\{211\}$ planar channels. Shoulders are observed in the I yield for the $\{100\}$ and $\langle 110 \rangle$ scans and the width of these indicate that some I atoms occupy sites 0.35 ± 0.03 Å from $\{100\}$ planes and 0.67 ± 0.10 Å from $\langle 110 \rangle$ axes. These coordinates are consistent with the calculated location in the presence of a nearest-neighbor vacancy. A distribution between substitutional, random, and vacancy associated sites is considered and site occupancies are derived in a simultaneous fit to all five scans using an average potential model for channeling. The significance of these results in the light of previous hyperfine-field measurements is discussed.

I. INTRODUCTION

Recent interest in the environment of implanted atoms in metallic hosts has centered on the associated vacancy problem.[1] For implanted atoms too large to form pure substitutional solid solutions, a distribution of sites may be produced by association of the implanted atom with one or more of the mobile vacancies formed during the implantation process. Under certain conditions attachment to large clusters, loops of vacancies, or interstitials may occur. Recent lattice location experiments on Yb in Fe suggest that regular clusters of damage determine the implant location.[2]

Possible evidence for one or two vacancies bound to an implant atom has been found using Mössbauer spectroscopy for $5s$-$5p$ atoms in an Fe host.[3-5] In these experiments three unique hyperfine-field components were identified for the systems FeXe and FeI. These fields were interpreted as belonging to substitutional (high-field) sites, single-vacancy bound (intermediate-field) sites and two or more vacancy bound (low-field) sites. This paper presents the first independent evidence for the existence of a regular interstitial site in iron for implanted iodine atoms.

In an experiment in which the backscattering yield of a well-channeled beam is observed as the incident beam angle ψ_i is varied, the impurity and host yield curves show the same angular characteristics such as half-width and depth providing that the impurity atoms occupy substitutional sites in the lattice.[6] When regular interstitial sites are occupied the impurity angular yield $\chi_{imp}(\psi_i)$ may exhibit a specific "nonsubstitutional" structure depending on the site symmetry.[7,8] In a previous extensive investigation[9] of the location of implanted Br in Fe using the channeling technique, calculated angular distributions were used to fit the impurity angular yield structure in order to identify the oc-

cupancy and coordinates of the interstitial Br site. In the present FeI channeling experiment the impurity yields have been similarly interpreted using an analytical model, but the data have been tested for their consistency with specific sites deduced from recent calculations[10] using a vacancy cluster model.

Angular scans have been carried out across two major bcc crystal axes and three major planes using backscattered 3.5-MeV ^{14}N ions. $\langle 111 \rangle$ and $\{100\}$ scans had earlier been performed by de Waard and Feldman[11] using 2.0-MeV ^{4}He ions and although general agreement is found with their results, a more precise measurement of the I yield curves has been made by taking more data points in smaller angular steps so as to elucidate any structure. The narrowed central dips in the $\langle 110 \rangle$ and $\{100\}$ impurity backscattering yields are shown to be consistent with I atoms in interstitial sites caused by the presence of a nearest-neighbor vacancy. A site distribution is found which gives the best simultaneous fit to all five scans. Finally, the channeling results are compared with the recent interpretations of Mössbauer and nuclear magnetic resonance of oriented nuclei (NMRON) experiments.

II. EXPERIMENTAL

A. Sample preparation

The 99.999%-purity, zone-refined Fe single crystals used in this work were obtained from Materials Research Corporation in the form of 6-mm-diam rods and were cut into 1-mm-thick discs perpendicular to a $\langle 110 \rangle$ axis. These were then spark planed and electropolished in an electrolyte[12] containing 50-ml perchloric acid to 1000-ml glacial acetic acid. Iodine implantation was carried out at room temperature on the Harwell Mk IV separator using singly charged 140-keV ^{127}I ions. This energy is the same as that used for the radioactive

samples prepared by Drentje for the Groningen, Mössbauer,[3-5] and Oxford nuclear orientation[13] experiments. In order to avoid implant channeling and a consequent anomalous implant depth distribution, the crystals were tilted to an angle of $\sim 7°$ between the $\langle 110 \rangle$ and beam directions. The doses used were 5×10^{14} atoms cm^{-2}. A measurement of the projected range and straggling (Sec. II C) gave

$$\bar{R}_p = 210 \pm 50 \text{ Å}$$

and

$$\Delta \bar{R}_p = 90 \pm 30 \text{ Å (standard deviation)},$$

so that the average local concentration of I atoms in the implanted region was 0.27 at.%.

B. Experimental arrangement

^{14}N ions of several MeV have certain advantages over lighter ions when used as the backscattering probe in channeling experiments. These include both a reduction in pile-up impurity peak background[9] and a higher angular resolution because of the variation as $\sqrt{Z}$ of $\psi_{1/2}$, the half-width at half-maximum channeling depth. A beam of 3.5 MeV ^{14}N$^+$ ions collimated to 1 mm diam and $\pm 0.03°$ divergence was used on the Harwell 5-MeV Van de Graaff channeling facility. This has already been described elsewhere.[9,14] Crystal alignment was performed using the remote-controlled three-axis goniometer whose stepping motors allow adjustments of 0.01°. Backscattered particles were detected at $\pm 165°$ using two 100-mm^2 ORTEC Si surface-barrier detectors at 10 cm from the target. These had energy resolution for ^{14}N particles of 70 keV full width half-maximum (FWHM). Blocking effects for the scattered particles were avoided by careful choice of crystal alignment and scan coordinates.

C. Experimental results

Figure 1 shows a typical energy spectrum for ^{14}N backscattering from 5×10^{14} cm^{-2} FeI. Windows
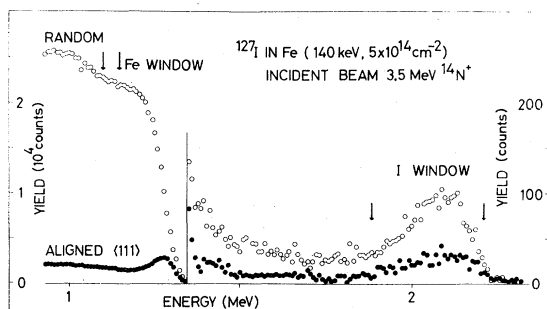
FIG. 1. Backscattered energy spectra for 3.5-MeV ^{14}N$^+$ ions incident in $\langle 111 \rangle$ and random directions in an Fe single crystal implanted with I. In the high-energy region the vertical scale has been expanded. The integrated target current was the same in both cases.

TABLE I. Experimental minimum backscattering yields and half-angles (half-width–half-dip) for both I and Fe in angular scans using 3.5-MeV ^{14}N.

Channel	$\chi_I(0)$	$\chi_{Fe}(0)$	$\psi^I_{1/2}$	$\psi^{Fe}_{1/2}$	Tilting plane
$\langle 111 \rangle$	0.36 ± 0.03	0.08	1.55 ± 0.10	1.55	20° from {110}
$\langle 110 \rangle$	0.36 ± 0.03	0.12	1.10 ± 0.07	1.15	14° from {110}
$\{110\}$	0.62 ± 0.02	0.46	0.60 ± 0.04	0.65	8° from $\langle 110 \rangle$
$\{100\}$	0.80 ± 0.01	0.69	0.35 ± 0.04	0.46	8° from $\langle 110 \rangle$
$\{211\}$	0.74 ± 0.02	0.68	0.30 ± 0.04	0.40	8° from $\langle 110 \rangle$

were set as shown, where the energy of the Fe window corresponds to scattering from the implant depth. This was determined from the difference between the I peak energy and the energy of scattering from the surface I nuclei of a KI crystal. Values for the stopping power of ^{14}N ions in Fe were taken from Ref. 15. The I yields were corrected for background, and by using an unimplanted crystal, it was verified that there were no other impurity peaks in the region of the I window. All spectra were accumulated at beam currents between 0.5 and 2.0 nA, the adjustment being made to keep the pile-up background approximately constant. Typical integrated charges of 3 μC on the ~ 1-mm-diam beam spot were used.

Angular scans were made for the $\langle 111 \rangle$ and $\langle 110 \rangle$ axes and the $\{100\}$, $\{110\}$, and $\{211\}$ planes. Table I shows the Fe and I minimum yields (χ_0) and Fe and I half-angles ($\psi_{1/2}$) using the 5×10^{14}-cm^{-2} FeI crystal. Figure 2 shows the complete scans. The ratios of the Fe angular widths for the two axes and three planes are in reasonable agreement with channeling theory[16] and their magnitudes agree well with previously published data.[6,9] As seen in Table I, the $\{100\}$ and $\{211\}$ planar scans exhibit considerably narrowed impurity yield curves. In examining specific structure it is clear from Fig. 2 that the $\{100\}$ and $\langle 110 \rangle$ I yields have shoulders about a central narrowed dip. These dips have half-widths $0.22° \pm 0.02°$ and $0.16° \pm 0.04°$, respectively. In both these scans there is a clear symmetry observed about $\psi_i = 0$.

III. INTERPRETATION OF THE DATA

A. Analytical model for channeling

The average-potential model used here for flux distribution calculations is essentially the same as that described in Ref. 9. Standard Lindhard row and plane potentials[16] have been used. A particle with initial transverse kinetic energy $E\psi_i^2$ entering at a position $\vec{\rho}_i$ (or y_i) in an axial (or planar) channel is constrained to oscillate within an equipotential contour with boundaries set by the initial transverse-energy conditions. Minimum distances of approach r_m (or y_m) to the boundary strings (or
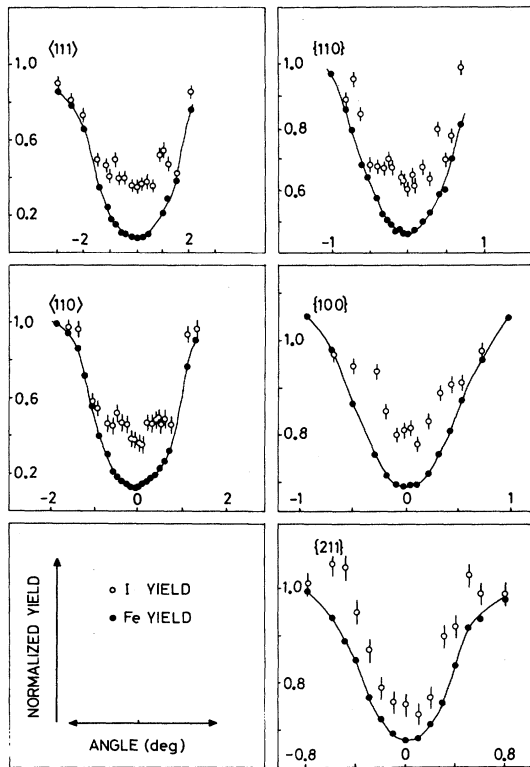
FIG. 2. Angular scans across the $\langle 111 \rangle$, $\langle 110 \rangle$, $\{110\}$, $\{100\}$, and $\{211\}$ channels in I-implanted Fe single crystals with 3.5-MeV $^{14}N^+$ ions. The I and Fe yields have been normalized to the random values. The smooth curves drawn through the Fe points are only to guide the eye.

planes) are then defined. In calculating r_m for axial channeling a numerical solution is found for the transverse-energy equation using a channel potential $U(\vec{\rho})$, which allows for four boundary strings. In the planar calculations there exists a simple analytic two-plane solution for y_m.

For axial channeling, the flux at position $\vec{\rho}$ is given by

$$F(\vec{\rho}) = \int\int_{A_0} f(\vec{\rho}, r_m(E, \psi_i, \vec{\rho_i})) \, dA(\vec{\rho_i}), \qquad (1)$$

where the integral is taken over the channel area A_0. A similar integral, in this case one dimensional, is used for the planar flux calculation. The individual particle axial and planar flux probabilities $f(\vec{\rho}, r_m)$ and $f(y, y_m)$ are according to the statistical-equilibrium approach of Lindhard.[16] All integrations were performed numerically as part of an ALGOL channeling program written for the Oxford University I.C.L. 1906A computer. No allowance has been made in the program for thermal vibrations, multiple scattering, or beam divergence effects. However, previous comparisons with the results of the Monte Carlo simulations,[9] which take

account of these effects, have shown that their presence merely acts to smooth somewhat the calculated angular yield structure. Of more concern is the assumption of statistical equilibrium inherent in the analytical model. While depth-dependent effects are clearly important, the large implant straggling length gives in effect a flux sampling over depth akin to the predictions of statistical equilibrium.

B. Sites for the I atoms

Any narrowing of impurity angular yield dips over the half-width defined by the host yield curve is consistent only with the occupation by at least a fraction of the impurity atoms of a nonsubstitutional location. Furthermore, it is necessary that these nonsubstitutional sites have some definite symmetry in the lattice since the effect of "randomly" placed impurity atoms whose scattering yield is independent of beam angle is to make the yield curve shallower but not to alter its half-width or shape from that exhibited by the host.

Using the model described in Sec. III A it was shown that the central dip widths in the $\{100\}$ planar and $\langle 110 \rangle$ axial channels correspond to the occupation by some I atoms of a site 0.35 ± 0.03 Å from $\{100\}$ planes (in a $\langle 100 \rangle$ direction) and at a radius of 0.67 ± 0.10 Å from $\langle 110 \rangle$ axes. Since these distances derive from the central angular scan structure, they locate the sites most central in their respective channels.

Drentje and Esker[10] have made computer calculations of the lattice positions for Xe atoms in bcc Fe in the vicinity of vacancies. The screened Thomas-Fermi potentials used in the model are only slightly different for the case of FeI, so the site positions should apply in the present analysis. Site occupancies are more difficult to ascertain since these depend strongly on the calculated formation energy and the distribution of damage. The site most easily formed, however, is the first-nearest-neighbor vacancy $V_1(1)$, requiring 8.5 eV, while the next most probable sites are $V_2(1)$, the second-nearest-neighbor vacancy (10.0 eV) and $V_1(2)$, the two nearest-neighbor vacancy configurations (11.2 eV). $V_2(1)$ is so similar to a substitutional site, as regards channeling, that only $V_1(1)$ and $V_1(2)$ are of interest here. Both configurations are illustrated in Fig. 3. Figure 4 shows the projection of all physically equivalent $V_1(1)$ and $V_1(2)$ sites viewed down the major axial and planar channels. The distance from the channel wall of the site $V_1(1)$ most central in the $\{100\}$ channel is 0.36 Å, while the most central $\langle 110 \rangle$ $V_1(1)$ site is 0.62 Å from the nearest boundary. Both these results are in excellent agreement with the central structure in the $\{100\}$ and $\langle 110 \rangle$ scans. In contrast, the $V_1(2)$ site gives 0.60 and 0.63 Å for these two distances.

Yield calculations for all five scans have been

$\odot = I$ $O = $ VACANCY $\bullet = $ Fe
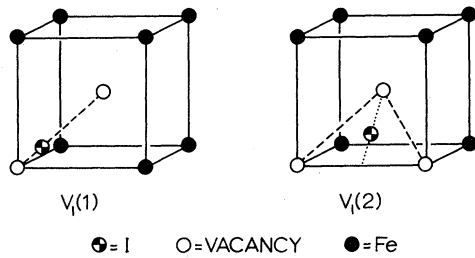
FIG. 3. Proposed sites for implanted I in Fe based on calculations by Drentje and Ekster (Ref. 10) for Xe in Fe. In $V_1(1)$ the I atom is shifted $\frac{1}{4}$ of the distance towards the nearest-neighbor vacancy. In $V_1(2)$ it sits at the center of the triangle formed by the two nearest-neighbor vacancies and the site vacated by the I atom.

carried out by allowing for site distribution of the following types.

(a) Substitutional I atoms for which the angular yields $\chi_s(\psi_i)$ must be identical to the experimental host yield $\chi_{Fe}^{expt}(\psi_i)$.

(b) Randomly distributed I atoms (associated perhaps with severe local damage) for which the angular yields $\chi_R(\psi_i)$ must equal unity.

(c) Interstitial I atoms of the $V_1(1)$ and $V_1(2)$ types whose yields $\chi_i(\psi_i)$ are calculated as follows. An allowance is made for the fraction of the beam undergoing uncorrelated motion in the lattice (the random beam) due to dechanneling in the damaged Fe. (The yield calculations implicitly take into account the unchanneled beam fraction $\chi_i^{calc}(\psi)$ arising from the surface transmission.) The fraction of the initially channeled beam which has become dechanneled is[9]

$$f_R = \frac{\chi_{Fe}^{expt}(0) - \chi_{Fe}^{calc}(0)}{1 - \chi_{Fe}^{calc}(0)}, \qquad (2)$$
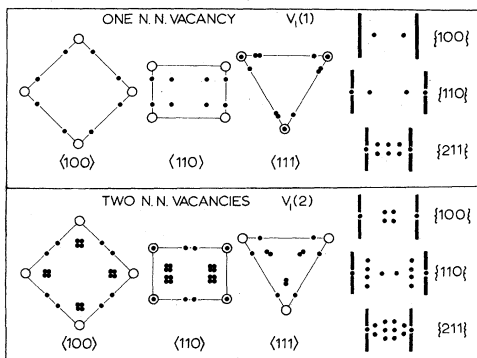
FIG. 4. Projections of the various physically equivalent $V_1(1)$ and $V_1(2)$ sites on planes normal to $\langle 100 \rangle$, $\langle 110 \rangle$, and $\langle 111 \rangle$ axial channels and $\{100\}$, $\{110\}$, and $\{211\}$ planar channels in Fe. Open circles in the case of the axes and lines in the case of the planes denote rows and planes of Fe atoms, respectively.
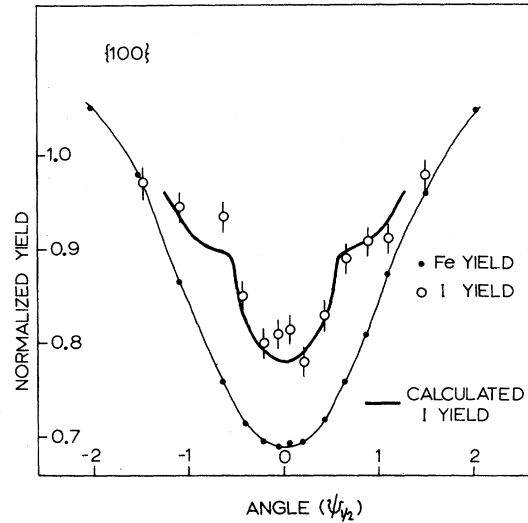
FIG. 5. Comparison between the calculated yield curve and the experimental $\{100\}$ scan. The computed I yield is a best fit for the $\{100\}$ scan alone for which the occupancy parameters are found to be $a_s = 0.55$, $a_1 = 0.30$, $a_2 = 0$, $a_R = 0.15$. The central I dip width of $0.25°$ determines the position of the central interstitial projection to be 0.35 Å from the center of the $\{100\}$ plane.

where the superscripts denote experimental and calculated quantities. f_R was typically 0.1 for axes and 0.2 to 0.5 for planes. For interstitial atoms the calculated yield $\chi_i^{calc}(\psi)$ is corrected to give

$$\chi_i(\psi) = (1 - f_R)\chi_i^{calc}(\psi) + f_R . \qquad (3)$$

The net yield may then be written

$$\chi(\psi) = a_s\chi_s(\psi) + a_R + a_1\chi_{V_1(1)}(\psi) + a_2\chi_{V_1(2)}(\psi), \qquad (4)$$

where the a's are the respective site occupancies. a_2 has been set equal to zero in the first instance. Figure 5 shows the $\{100\}$ scan with the I yield fitted for the three parameters a_s, a_R, a_1, where the best fit is $a_s = 0.55$, $a_1 = 0.30$, $a_2 = 0.0$, $a_R = 0.15$. A simultaneous fit to the five scans calculated for the most compatible set of occupancies ($a_s = 0.6$, $a_1 = 0.2$, $a_2 = 0.0$, $a_R = 0.2$) is shown in Fig. 6 along with the curves obtained when a_1 and a_2 are set equal to unity. None of the data suggest that an improved fit would result if a_2 were nonzero. There is insufficient sensitivity to the presence of I atoms with two nearest-neighbor vacancies.

IV. DISCUSSION

Confidence in the yield structure interpretation must be tempered by a recognition of the weaknesses of the analytical model for channeling. The assumption of statistical equilibrium, the lack of any allowance for correlated motion in the transverse plane,[17] and the absence of multiple scatter-
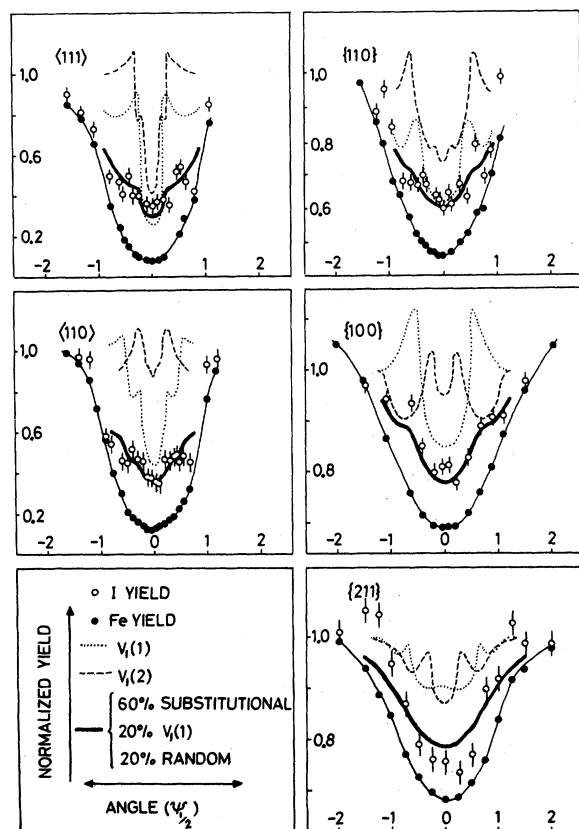
FIG. 6. Simultaneous fits to the I angular yield curves for the $\langle 111 \rangle$, $\langle 110 \rangle$, $\{110\}$, $\{100\}$, and $\{211\}$ scans. The thick solid line is the calculated fit to the experimental I yield using a single set of occupancy parameters $(a_s = 0.6, a_1 = 0.2, a_2 = 0, a_R = 0.2)$. For comparison, the dotted and dashed lines show the calculated curves for I atoms exactly in $V_1(1)$ and $V_1(2)$ locations. No improvement in fit results from allowing I atoms to occupy $V_1(2)$ sites. All calculated curves are corrected for the random beam fraction according to Eq. (3).

ing effects are sources of uncertainty in the analysis. This uncertainty must be reflected in the derivation of the site occupancies, but has little influence on the identification of the $V_1(1)$ interstitial site by its coordinates in the $\{100\}$ and $\langle 110 \rangle$ channels. Here the channel potential used is important, but the Lindhard potentials are sufficiently accurate for estimates within the scale of present experimental errors.

Spectral line intensities in a Mössbauer experiment can give information about the fraction of impurity nuclei experiencing each hyperfine-field component in a distributed site system. Low-temperature recoilless fractions must, however, be obtained for each component before occupancy can be determined. De Waard et al.[18] have distinguished three hyperfine-field components for Fe ^{125}I (10^{15} cm^{-2}, 120 keV dose and implant energy) and Fe ^{131}I (3×10^{14} cm^{-2}, 120 keV) although the occupancies determined include no allowance for the presence of I atoms in sites with zero recoilless fractions. Later work by Reintsema and De Waard[5] on Fe ^{133}Xe has shown that a significant fraction of impurity atoms occupy such sites, presumably associated with a large number of vacancies. In their interpretation they took the I and Xe intermediate-field sites to be of the $V_1(1)$ type while the low-field component was taken to correspond with a greater number of vacancies in the vicinity of the impurity atom. The high-field fraction would include substitutional impurities and those with vacancies at next-nearest-neighbor or more distant locations. (Angular yield calculations show these to be indistinguishable in a channeling experiment.)

Table II gives a summary of the I and Xe Mössbauer and NMRON results. There is agreement between the high-field fractions for FeXe and the substitutional fraction (0.45) obtained from the χ_0

TABLE II. Site fractions as determined by recent Mössbauer and nuclear orientation experiments.

Experiment	Dose,	Energy (keV)	Fractions in various hyperfine fields			Zero recoilless fraction
			High	Intermediate	Low	
Fe ^{131}I[18] Mössbauer	3×10^{14},	120	0.39 ± 0.20[a]	0.31 ± 0.14[a]	0.30 ± 0.15[a]	?
Fe ^{125}I[18] Mössbauer	10^{15},	120	0.46 ± 0.05[a]	0.32 ± 0.04[a]	0.22 ± 0.06[a]	?
Fe ^{133}Xe[5] Mössbauer	10^{14},	140	0.33 ± 0.05	0.12 ± 0.04	0.14 ± 0.03	0.41 ± 0.07
Fe ^{131}I[13] NMR ON	10^{14},	140	$> 0.42 \pm 0.02$	$\cdots$	$\cdots$	$\cdots$
Fe $^{131}Xe^m$[19] Nuclear Orientation	3.5×10^{15},	75	0.45 ± 0.05	$\cdots$	$\cdots$	$\cdots$

[a]These fractions would be reduced if allowance were made for occupation of a site with zero recoilless fraction.

measurements of Feldman and Murnick.[20] In the case of FeI the high-field fraction is somewhat less than that obtained from the channeling experiment, the fraction of $V_1(1)$ atoms agrees fairly well with that obtained for the intermediate-field occupancy. It is quite reasonable that the more complex vacancy configurations grouped together under the titles "low field" and "zero recoilless fraction" may, in terms of their contribution to the total angular yield in a channeling experiment, be described as "random."

Direct evidence has been given by this experiment for the existence of implanted I atoms in an interstitial site in Fe whose location has been shown to correspond with that expected when a nearest-neighbor vacancy is present. Despite the difficulty in accurately determining site fractions in a chan-neling experiment, there appears to be reasonable agreement with the results of recent Mössbauer and nuclear orientation experiments.

ACKNOWLEDGMENTS

The authors are grateful to P. Kittel for rewriting the channeling program for use on the fast computer. We wish to thank H. de Waard and S. Drentje of the Physics Department, University of Groningen for valuable help in preparing radioactive samples and for useful discussions of the results. We also thank G. Read for his help in crystal preparation, G. Gard for performing the inactive implantations at AERE, Harwell, and T. Sparrow and the operating staff of the Harwell 5 MeV Van de Graff for making the experiment possible.

*Work supported by a grant from the United Kingdom Science Research Council.

†Present address: Department of Chemistry, Biochemistry, and Biophysics, Massey University, Palmerston North, New Zealand.

[1] H. de Waard, *Mössbauer Spectroscopy and Its Applications* (IAEA, Vienna, 1972), p. 123.

[2] F. Abel, M. Bruneaux, and C. Cohen, Solid State Commun. 13, 113 (1973).

[3] H. de Waard and S. A. Drentje, Phys. Lett. 20, 38 (1966).

[4] H. de Waard and L. C. Feldman, *Applications of Ion Beams to Metals* (Plenum, New York, 1974), p. 317.

[5] S. R. Reintsema, S. A. Drentje and H. de Waard, contributed papers at the International Conference on Hyperfine Interactions, Uppsala, 1974 (unpublished), p. 74.

[6] R. B. Alexander and J. M. Poate, Radiat. Eff. 12, 211 (1972).

[7] R. B. Alexander, G. Dearnaley, D. V. Morgan, and J. M. Poate, Phys. Lett. A 32, 365 (1970).

[8] J. U. Andersen, O. Andreasen, J. A. Davies, and E. Uggerhøj, Radiat. Eff. 7, 25 (1971).

[9] R. B. Alexander, P. T. Callaghan, and J. M. Poate, Phys. Rev. B 9, 3022 (1974).

[10] S. A. Drentje and J. Ekster, Internal report, Natuurkunding Laboratorium, Groningen, 1969 (unpublished).

[11] H. de Waard and L. C. Feldman, *Applications of Ion Beams to Metals* (Plenum, New York, 1974), p. 340.

[12] W. J. McG. Tegart, *The Electrolytic and Chemical Polishing of Metals in Research and Industry*, 2nd ed. (Pergamon, London, 1959).

[13] P. K. James, N. J. Stone, and H. R. Foster, Phys. Lett. A 48, 237 (1974).

[14] K. C. Knox, Nucl. Instrum. Methods 81, 202 (1970).

[15] L. C. Northcliffe and R. F. Schilling, Nucl. Data A 7, 233 (1970).

[16] J. Lindhard, Mat-Fys. Medd. Dan. Vid. Selsk. 34, No. 14 (1965).

[17] J. H. Barrett, Phys. Rev. B 3, 1527 (1971).

[18] H. de Waard, R. L. Cohen, S. R. Reintsema, and S. A. Drentje, Phys. Rev. B 10, 3760 (1974).

[19] H. Pattyn, R. Coussement, G. Dumont, E. Schueters, R. E. Silverans, and L. Vanneste, Phys. Lett. A 45, 131 (1973).

[20] L. C. Feldman and D. E. Murnick, Phys. Rev. B 5, 1 (1972).